Variations in the Extent of Pyrochlore-Type Cation Ordering in Ce 2 Zr 2 O 8 : A t'−κ Pathway to Low-Temperature Reduction

8 AUTHORS, INCLUDING:

Paolo Fornasiero
Università degli Studi di Trieste
236 PUBLICATIONS **8,749** CITATIONS

SEE PROFILE

Miguel Banares
Spanish National Research Council
211 PUBLICATIONS **4,330** CITATIONS

SEE PROFILE

Ivano Alessandri
Università degli Studi di Brescia
58 PUBLICATIONS **610** CITATIONS

SEE PROFILE

Laura E. Depero
Università degli Studi di Brescia
334 PUBLICATIONS **3,730** CITATIONS

SEE PROFILE

Variations in the Extent of Pyrochlore-Type Cation Ordering in Ce₂Zr₂O₈: A t′−κ Pathway to Low-Temperature Reduction

T. Montini,[†] N. Hickey,[†] P. Fornasiero,*,[†] M. Graziani,[†] M. A. Bañares,[‡]
M. V. Martinez-Huerta,[‡] I. Alessandri,[§] and L. E. Depero[§]

*Center of Excellence for Nanostructured Materials, INSTM-Trieste and Chemistry Department,
via L. Giorgieri 1, Trieste, I-34127, Italy, Instituto de Catalisis y Petroleoquimica, CSIC, Marie Curie, 2,
E-28049, Madrid, Spain, and INSTM and Laboratorio di Chimica per le Tecnologie, University of Brescia,
via Branze 38, I-25123, Brescia, Italy*

A Ce₂Zr₂O₈ mixed oxide was prepared, and the influence of redox treatments on its reduction behavior was systematically analyzed. The temperature of reduction was found to change on application of redox cycles under severe conditions, with the final appearance of temperature-programmed reduction profiles dictated by the exact conditions employed in the redox cycle (temperature of treatment and concentration of H₂). In addition, the conditions necessary in the reducing and oxidizing parts of the redox cycle showed interdependence. The reduction was found to vary from a single high-temperature peak to a single low-temperature peak, via double-peak profiles with various relative intensities. Structural analysis of the sample after application of analogous treatments indicated that the reduction behavior follows a pathway, with t′ and κ phases at the two extremes (high- and low-temperature single-peak profiles). The latter phase contains pyrochlore-type cation ordering. However, bulk ordering is not necessary to promote low-temperature reduction. The evidence suggests that the two-peak profiles are observed when cation ordering is very limited, and a single low-temperature peak is observed when domains of the κ phase coexist with larger amounts of the t′ phase. Thus, even the presence of partial ordering at the surface is sufficient to produce an effect.

1. Introduction

The redox properties of ceria−zirconia mixed oxides (CZMOs) have attracted widespread scientific interest in catalysis: as electrolyte materials for solid oxide fuel cells (SOFCs);[1,2] as supports in catalysts for the generation and purification of H₂;[3] but most notably for their use in automotive three-way catalysts (TWCs), in which CZMOs are included as a standard component to promote the oxygen storage capacity (OSC) of the catalyst.[4] This aspect alone has generated an enormous amount of research into the redox properties of CZMOs.[4,5] The search for a correlation between structure and reduction performance has been a common approach to such investigations, and the $Ce_{1−x}Zr_xO_2$ phase diagram has been extensively studied.[6] At high ceria content ($x \leq 0.15$), a cubic phase is formed, which presents the fluorite structure of CeO₂ ($Fm3m$), while at very low ceria content ($x \geq 0.85$), a monoclinic phase is found. For $0.15 \leq$ $x \leq 0.85$, three tetragonal forms are generally reported: t, t′, and t″. The thermodynamically stable t phase is formed at high zirconia content ($0.7 \leq x \leq 0.85$), while the metastable t′ phase ($P4_2/nmc$) is formed in the composition range $0.35 \leq x \leq 0.7$. Finally, the t″ or pseudocubic phase (also metastable) is intermediate between the t′ and c phases ($0.15 \leq x \leq 0.35$ or $0.15 \leq x \leq 0.5$ for small particles). This is characterized by a cubic ($Fm3m$) cation sublattice, while its oxygen sublattice is tetragonally distorted ($P4_2/nmc$). Because of the variable valence character of CZMOs, oxygen-deficient structures may also be formed under reducing conditions.[7,8] The pyrochlore structure is represented by the general formula $A_2B_2X_7$, where A and B are cations arranged in a face-centered cubic structure and X represents anions in tetrahedral sites within this arrangement. In the ideal structure, which is strictly related to that of fluorite, $^1/_8$ of the anions are absent in a systematic way and it may thus be considered as an ordered defect structure ($Fd3m$).[7,9] However, pyrochlores are usually not fully stoichiometric and are therefore often represented as $A_2B_2X_{7+y}$. The pyrochlore structure in CZMOs is usually reported to form at high temperature under reducing conditions.[7,10,11]

* Corresponding author. Phone: +39 040 5583973. Fax: +39-040-5583903. E-mail: pfornasiero@units.it.
† Center of Excellence for Nanostructured Materials.
‡ Instituto de Catalisis y Petroleoquimica.
§ University of Brescia.

(1) Kawamura, K.; Watanabe, K.; Hiramatsu, T.; Kaimai, A.; Nigara, Y.; Kawada, T.; Mizusaki, J. *Solid State Ionics* **2001**, *144*, 11.
(2) Izu, N.; Kishimoto, H.; Omata, T.; OtsukaYaoMatsuo, S. *J. Solid State Chem.* **2000**, *151*, 253.
(3) Montoya, J. A.; RomeroPascual, E.; Gimon, C.; DelAngel, P.; Monzon, A. *Catal. Today* **2000**, *63*, 71.
(4) Kaspar, J.; Fornasiero, P.; Graziani, M. *Catal. Today* **1999**, *50*, 285.
(5) Kaspar, J.; Fornasiero, P.; Hickey, N. *Catal. Today* **2003**, *77*, 419.
(6) Yashima, M.; Hirose, T.; Katano, S.; Suzuki, Y.; Kakihana, M.; Yoshimura, M. *Phys. Rev. B* **1995**, *51*, 8018.

(7) Thomson, J. B.; Armstrong, A. R.; Bruce, P. G. *Chem. Commun.* **1996**, 1165.
(8) Thomson, J. B.; Armstrong, A. R.; Bruce, P. G. *J. Am. Chem. Soc.* **1996**, *118*, 11129.
(9) Tabira, Y.; Withers, R. L.; Minervini, L.; Grimes, R. W. *J. Solid State Chem.* **2000**, *153*, 16.
(10) Otsuka-Yao-Matsuo, S.; Omata, T.; Izu, N.; Kishimoto, H. *J. Solid State Chem.* **1998**, *138*, 47.

An aspect of the reduction behavior of CZMOs which has received considerable attention is the unusual reversible redox behavior that these materials exhibit on application of severe oxidizing and reducing treatment procedures.[10–13] A number of investigations have reported that the Ce:Zr = 1:1 composition ($Ce_2Zr_2O_8$) shows the lowest temperature reduction across the range of CZMOs.[14,15] More recently, two new phases, designated κ and t*, have been reported and characterized for this composition.[11,16–20] The results obtained for the κ phase offer convincing evidence that its structure favors low-temperature reduction.[10,11] It is formed by controlled oxidation of a pyrochlore precursor. This material shows promoted reduction as long as the temperature of oxidation is low enough to maintain the cation ordering of the precursor. High-temperature oxidation results in formation of the t* phase, which no longer exhibits promoted reduction. According to one report of structural analysis, the cation ordering is maintained during low-temperature reoxidation, with slight shifts in positions, resulting in a structure with the $P2_13$ space group.[17] However, another report has suggested that this model may not be entirely correct.[21] The latter has been supported by theoretical studies.[15] This debate underlines a frequently encountered problem in structural analysis of these materials. Even when well-crystallized phases are present, it is difficult to establish the structure with certainty. In addition, the metastable phases formed at intermediate compositions, with consequent facile phase separation, further complicate the situation. In a neutron-diffraction study, Mamontov et al. have reported that microdomains of either zirconium- or cerium-enriched phases, not detectable by X-ray diffraction, are responsible for improved oxygen release characteristics of a $Ce_2Zr_2O_8$ material.[22] In such cases, average or main phases may be detected by conventional structural analysis.

As noted above, the pyrochlore structure is usually reported to form under rather severe reducing conditions. However, in a recent rapid communication we reported evidence for its formation at low temperature during promoted reduction,[23] an observation strongly dependent on the treatment conditions employed. Here we report further evidence of the phenomenon and offer a more in-depth structural investigation.
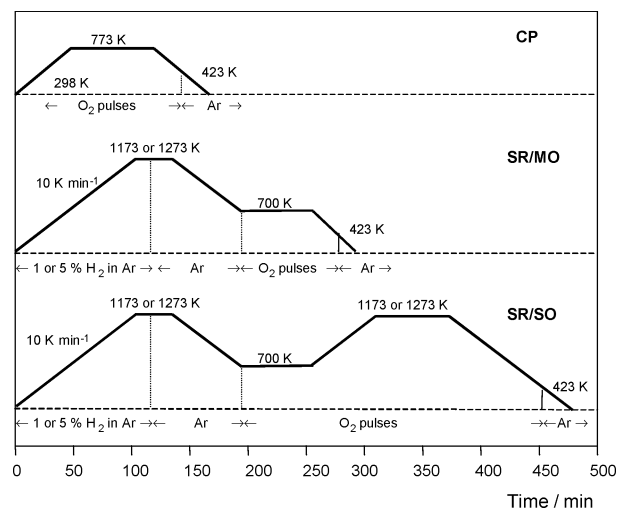

Figure 1. Schematic of treatment regimes employed. SR = severe reduction, SO = severe oxidation, MO = mild oxidation.

2. Materials and Methods

$Ce_2Zr_2O_8$ was prepared by a citrate complexation route. An aqueous solution of cerium and zirconium nitrates (Aldrich 99.99%, 40 g L^{-1} of the final oxide) was stirred for 1 h at 348 K before complexation with citric acid (Fluka), with a citric acid:cation molar ratio of 2.1:1. The resulting system was stirred for 5 h at 348 K and then overnight at room temperature (rt), after which the solvent was removed using a rotary evaporator. The resin produced was dried overnight at 348 K and then calcined for 5 h at 773 K (ramp rate = 3 K min^{-1}). The Brunauer–Emmett–Teller surface area was 40 m^2 g^{-1}. Surface area measurements were conducted by N_2 adsorption at 77 K on a Micromeritics ASAP instrument.

Temperature-programmed reduction (TPR) profiles were recorded in flow systems equipped either with a thermal conductivity detector (TPR-TCD) or a VG Sensorlab quadrupole mass spectrometer detector (TPR-MS). The cleaning/redox procedures applied to the sample are illustrated in Figure 1. An in situ cleaning procedure (CP) was applied before each set of experiments. This consisted of oxidizing the sample at 773 K, holding for 1 h, then cooling, first to 423 K oxygen, then to rt in Ar. After CP, aliquots of the sample were subjected to a series of redox cycles consisting of TPR (severe reduction, SR) followed by intermediate oxidation steps (severe oxidation, SO, or mild oxidation, MO). The TPR profiles were obtained by heating the sample from rt (30 min) to 1173 or 1273 K in 1 or 5% H_2/Ar, holding for 15 min, then switching to Ar (15 min). After TPR, the samples were cooled to 700 K in Ar, oxidized for 1 h, and then either cooled to rt (SR/MO) or oxidized for 2 h at the final TPR temperature of 1173 or 1273 K (SR/SO). Because of differences in the experimental setup of the two systems, oxidation was conducted by O_2 (100%) pulses in TPR-TCD (100 μL, every 75 s) and under O_2 flow (5% in Ar) in TPR-MS. In all cases flow and ramp rates were 25 mL min^{-1} and 10 K min^{-1}, respectively. In the case of TPR-MS, a heated capillary line was used to transfer the reactor outstream to the detector.

Powder X-ray diffraction (XRD) patterns were collected on a Philips 1830 PW diffractometer (Ni-filtered Cu Kα), at 2θ values from 10 and 100° in steps of 0.02°. The acquisition time at each step was usually 3 s, but in selected cases, this was increased to 12 s. Peak positions were calibrated using the always-present aluminum sample-holder reflections as reference.

(11) Omata, T.; Kishimoto, H.; OtsukaYaoMatsuo, S.; Ohtori, N.; Umesaki, N. *J. Solid State Chem.* **1999**, *147*, 573.
(12) Fornasiero, P.; Montini, T.; Graziani, M.; Kaspar, J.; Hungria, A. B.; MartinezArias, A.; Conesa, J. C. *PCCP* **2002**, *4*, 149.
(13) Baker, R. T.; Bernal, S.; Blanco, G.; Cordon, A. M.; Pintado, J. M.; Rodriguez-Izquierdo, J. M.; Fally, F.; Perrichon, V. *Chem. Commun.* **1999**, 149.
(14) Fornasiero, P.; Di Monte, R.; Ranga Rao, G.; Kaspar, J.; Meriani, S.; Trovarelli, A.; Graziani, M. *J. Catal.* **1995**, *151*, 168.
(15) Conesa, J. C. *J. Phys. Chem. B* **2003**, *107*, 8840.
(16) Shinya, O. Y. M.; Omata, T.; Izu, N.; Kishimoto, H. *J. Solid State Chem.* **1998**, *138*, 47.
(17) Kishimoto, H.; Omata, T.; Otsuka-Yao-Matsuo, S.; Ueda, K.; Hosono, H.; Kawazoe, H. *J. Alloys Compd.* **2000**, *312*, 94.
(18) Nagai, Y.; Yamamoto, T.; Tanaka, T.; Yoshida, S.; Nonaka, T.; Okamoto, T.; Suda, A.; Sugiura, M. *Catal. Today* **2002**, *74*, 225.
(19) Sasaki, T.; Ukyo, Y.; Suda, A.; Sugiura, M.; Kuroda, K.; Arai, S.; Saka, H. *J. Ceram. Soc. Jpn.* **2003**, *111*, 382.
(20) Sasaki, T.; Ukyo, Y.; Kuroda, K.; Arai, S.; Saka, H. *J. Electron Microsc.* **2003**, *52*, 309.
(21) Sasaki, T.; Ukyo, Y.; Suda, A.; Sugiura, M.; Kuroda, K.; Arai, S.; Saka, H. *J. Ceram. Soc. Jpn.* **2003**, *111*, 382.
(22) Mamontov, E.; Brezny, R.; Koranne, M.; Egami, T. *J. Phys. Chem. B* **2003**, *107*, 13007.

(23) Montini, T.; Banares, M. A.; Hickey, N.; Di Monte, R.; Fornasiero, P.; Kaspar, J.; Graziani, M. *PCCP* **2004**, *6*, 1.

In situ TPR−Raman spectra were obtained on a Renishaw Raman System 1000, with an Ar laser (514 nm, 25 mW) fitted with a cell that allows control of temperature and gas flow. For in situ Raman spectra, a CP procedure, analogous to that used in TPR experiments, was applied before the start of any set of experiments. Reduction treatments were performed by introducing the reducing gas (1 or 5% H_2 in Ar,), heating in a stepwise manner (50 K intervals), and recording the spectra during the isothermal steps (15 min). Intermediate oxidation steps (5% O_2 in Ar) were performed in the same cell.

Fourier transfrom (FT)-IR spectra were collected at rt on a Perkin-Elmer 2000 FT-IR spectrometer with MCT detector using a static quartz cell. Samples were prepared by conducting ex situ redox treatments in the same apparatus used for TPR-TCD. The powdered samples thus prepared were pressed into self-supporting for FT-IR measurements. An in situ cleaning procedure, consisting of calcination with O_2 at 700 K (pressure = 300 mbar, time = 1 h) followed by evacuation at 700 K (1 h), was employed as a standard first step in all investigations. Methanol adsorption studies were conducted by exposure of the cleaned samples to methanol vapor (25 mbar, rt for 10 min) followed by evacuation for 1 h at 373 K, before cooling to room temperature to collect the IR spectra.

3. Results and Discussion

3.1. TPR. The ability to cycle between promoted and unpromoted reduction upon application of appropriate redox treatments is a well-established phenomenon in the redox behavior of CZMOs.[10−13] We have recently reported that, in addition to the known detrimental effect of SO on the subsequent TPR profile, other factors, such as H_2 concentration in the reduction step (1 vs 10% H_2 in Ar), may be used to control the onset of promoted reduction.[23] This was further investigated in a series of TPR experiments using variations in the SO and TPR (SR) procedures designed to identify the influence or relative importance of individual parameters on the promotion observed. Water evolution profiles during a typical series of experiments with 1 and 5% H_2/Ar are shown in Figure 2. It should be noted that for the first 5 pairs of profiles the maximum temperature of reduction is 1173 and 1273 K thereafter. The H_2 uptake profiles (not shown) correspond closely with the water evolution profiles, thereby indicating a correlation between H_2 uptake and sample vacancy creation.

In view of the fact that the reduction profile observed during TPR is a function of the H_2 concentration (higher concentration = lower temperature),[24] the data for 1 and 5% H_2 cannot be directly compared. After identical treatments, peak positions using 5% H_2 are invariably lower than those observed using 1% H_2. In addition, the fact that different concentrations of H_2 are used means that only for the first pair of TPRs have the samples undergone identical treatments. Thus, comparison of the effect of redox treatments within the same data set is the only valid approach. For both sets of data, it may be stated that, to see promotion of reduction with respect to that observed for the first or second TPR profile, it is necessary to subject the sample to a SO−SR−MO cycle. In the case of 5% H_2, this is clearly seen in profile 4 of Figure 2 (profile 3 being the SR of the
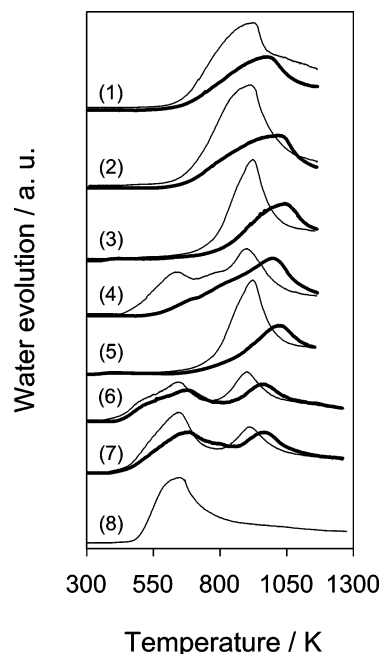
(24) Monti, D. A. M.; Baiker, A. *J. Catal.* **1983**, *83*, 323.

Figure 2. Water evolution during TPR profiles of Ce₂Zr₂O₈ using 1% H_2/Ar (bold lines) and 5% H_2/Ar as reducing agent. Profiles 1−7 were obtained consecutively, as follows: (1) after CP; (2) after 1−MO; (3) after 2−SO (1173 K); (4) after 3−MO; (5) after 4−SO (1273 K); (6) after 5−MO; (7) after 6−MO; (8) TPR of Ce₂Zr₂O₈ after SO (1273 K)−SR (1353 K, 5 h)−MO. CP, 773 K, 1 h; MO, 700 K, 1 h; SO, 2 h.

SO−SR−MO cycle); while for 1% H_2, a similar promotion is seen only in profile 6.

Within this general framework, the influence of individual parameters on the reduction behavior is evident. Thus, as we have previously reported,[23] there is an effect of H_2 concentration: when the SO and SR treatments are limited to 1173 K, significant low-temperature reduction is observed with 5% H_2 (profile 4); whereas only a slight promotion, in the form of a low-temperature shoulder, is observed with 1% H_2 (profile 4, bold). The importance of the temperature of oxidation in the phenomenon under discussion has been well-established, and there are various reports on the different response of analogous systems to mild and severe oxidation. Here, it is clear that the concept of mild or severe oxidation also depends on the other parameters in the SO−SR−MO cycle: with 1% H_2, it is necessary to oxidize the sample at 1273 K in order to see significant promotion after the subsequent SR−MO, as shown by profile 6, bold line. With 5% H_2, although SO (1173 K)−SR (1173 K)−MO significantly promotes reduction, there is further improvement on passing from SO (1173 K)−SR (1173 K) to SO (1273 K)−SR (1173 K), as seen from comparison of profiles 4 and 6 of Figure 2. The latter has a distinct shoulder at 500 K. Finally, profile number 8 shows the effect on the TPR profile of increasing the reduction temperature during a SO−SR−MO cycle with 5% H_2. A single, low-temperature peak results.

To accurately measure the degree of sample reduction achieved during individual TPR experiments, a parallel series of experiments was conducted using a TCD detector. The degree of sample reduction was measured from O_2 uptake during pulsed oxidation at 700 K after TPR experiments (see Figure 1). A more extensive set of experiments was
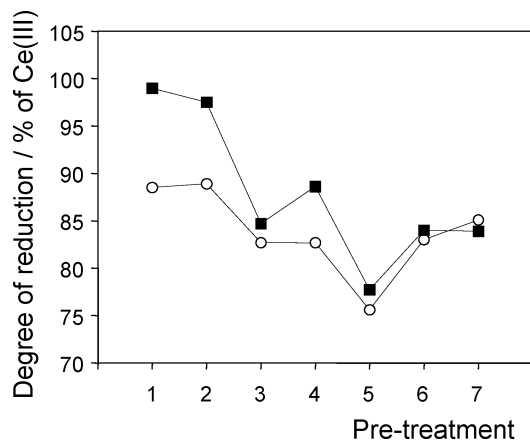
Figure 3. Degree of reduction of $Ce_2Zr_2O_8$ reached during TPR profiles corresponding to profiles 1−7 of Figure 2, as measured from O_2 uptake at 700 K after TPR-TCD. (■) 5% H_2/Ar and (○) 1%/Ar. The were obtained consecutively, under the same conditions as in Figure 2. The error in the measurements series of profiles reported has been calculated as ±1%.

performed in this case, using both 1 and 5% H_2 as for TPR-MS but with extra TPR(SR)−MO cycles. The profiles obtained agree remarkably well with those obtained in TPR-MS experiments (Figure 2). However, a further interesting point to emerge from these data (not shown here) is the effect of consecutive SRs when all parameters are held constant. With both 1 and 5% H_2, SO (1273 K)−SR (1173 K)−MO results in significant promotion of reduction, as in Figure 2. Subsequent SR (1173 K)−MO promotes the reduction even further: in each case, the relative intensity of the two-peak profiles shifts toward the low-temperature peak. Subsequent SR (1273 K)−MO had no additional effect. This may be taken to indicate that time of reduction is also an important factor. The process resulting in promotion thus appears to be relatively slow and is not completed within the time frame of the standard procedure used here.

The results of analysis of the degree of reduction after TPR-TCD are summarized in Figure 3. It should be noted that the promotion observed under TPR conditions, i.e., shifts to low temperature, is a kinetic promotion. Any differences in the degrees of reduction observed may also be attributed to kinetic factors. Particle size growth makes the samples more difficult to reduce, and reduction of aged samples, even to 1273 K, generally does not result in complete reduction. For the first pair of measurements, the higher degree of reduction observed using 5% H_2 is attributed to the higher H_2 concentration. By use of both 5 and 1% H_2, there is a general decrease in the degree of reduction observed across the first 5 pairs of measurements. This general trend may be partially attributed to the fact that throughout these measurements the particle size changes. In both series, the first two profiles show essentially the same degrees of reduction, while significant decreases are apparent after severe oxidation procedures. The effect of severe oxidation at 1273 K is greater than that at 1173 K. Oxidation at 1273 K is the highest thermal treatment used in 1−5, and a particle sintering effect, as demonstrated X-ray diffraction and surface area measurements (vide infra), almost certainly plays a role in this observation. However, an effect of structural modification cannot at present be excluded. The exception to the general downward trend is in the fourth measurement using

5% H_2: the higher degree of reduction reflects the promotion of reduction observed in the TPR profile 4 of Figure 2. The reduction observed in the last two sets of profiles does not change. For these profiles, there should be no further thermal evolution of the particle size and both have undergone treatments which lead to promoted reduction.

The data in Figure 3 suggest that promotion of reduction is not linked to the degree of reduction induced by the preceding SR. With 5% H_2, the sample is essentially reduced to $Ce_2Zr_2O_7$ during the first TPR, yet reduction is not promoted until the fourth, after application of SO 1173 K. Thus, more extensive reduction does not necessarily lead to promotion. The major difference in the TPR behavior in Figure 2 is the fourth pair of profiles: significant promotion is observed with 5% H_2, while it is very limited with 1% H_2. This is reflected in the difference in the degree of reduction reported in Figure 3. However, very similar degrees of reduction were observed in the third pair of profiles. Similarly, the degrees of reduction observed in the fifth pair, after SO at 1273 K, are also very similar and less extensive than observed after the third pair, after SO at 1173 K. In the subsequent measurements, both samples show promotion and similar degrees of reduction (6, Figures 2 and 3). Thus, for 5% H_2, quite a wide range of degree of reduction leads to subsequent promotion, while for 1%, even when the degree of reduction falls within this range, promotion is not necessarily observed. In the case of 1% H_2, the possibility existed that reduction and therefore subsequent promotion was limited by the H_2 concentration, although it should be noted that 100% H_2 uptake was never observed during TPR-MS when 1% H_2 was used as a reducing agent.

In conclusion, it may be stated that we have identified a number of parameters which may be tuned in order to influence the TPR behavior. Comparison of the TPR profiles using 5% H_2 with those previously published using 10% H_2[23] indicates that further promotion is possible using the procedures described: using 10% H_2, after SO(1273)−SR-(1273)−MO, a similar two-peak profile was obtained, with a much more intense lower temperature peak.

Having established the reduction behavior of the present sample by means of TPR, structural characterization of the sample was conducted after similar treatments to those employed in Figures 2 and 3 to gain insight into the profiles or identify any structure−TPR correlation.

3.2. Raman Spectroscopy. Extraction of structural information from Raman spectroscopy of CZMOs is potentially hampered by the possibility that the sample may contain trace impurities of rare-earth ions,[25] which may give rise to intense f−f luminescence superimposed on underlying Raman bands. In such cases, true structural information is not contained in the Raman part of the spectrum. To confirm or exclude this possibility, spectra should be recorded using different excitation energies. To this end, we recorded emission spectra of our $Ce_2Zr_2O_8$ material using three distinct excitation lines (1064, 632.8, and 514 nm). The results obtained (not shown) allow us to exclude the possibility that there are interfering

(25) Fornasiero, P.; Speghini, A.; Di Monte, R.; Bettinelli, M.; Kaspar, J.; Bigotto, A.; Sergo, V.; Graziani, M. *Chem. Mater.* **2004**, *16*, 1938.
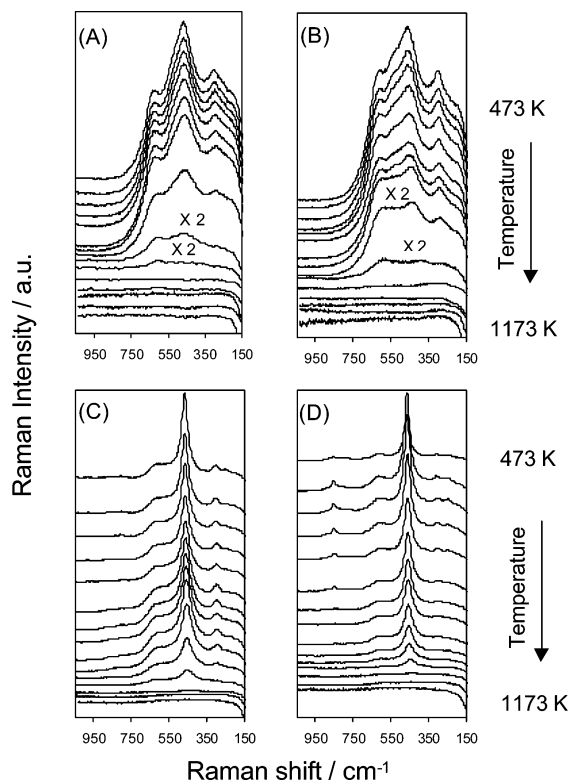
Figure 4. Consecutive series of in situ TPR−Raman spectra of $Ce_2Zr_2O_8$ obtained during reduction to 1173 K in 1% H_2/Ar: (A) after CP; (B) after A−MO; (C) after B−SO (1173 K); (D) after C−MO. Spectra were recorded at 50-K temperature intervals. The first spectrum in each case was recorded at 473 K. CP, 773 K, 1 h; MO, 700 K, 1 h; SO, 2 h.

Figure 5. Consecutive series of in situ TPR−Raman spectra of $Ce_2Zr_2O_8$ obtained during reduction to 1273 K in 5% H_2/Ar: (A) after CP; (B) after A−MO; (C) after B−SO (1273 K); (D) after C−MO. Spectra were recorded at 50 K temperature intervals. The first spectrum in each case was recorded at 473 K. CP, 773 K, 1 h; MO, 700 K, 1 h; SO, 2 h.

luminescence peaks at the excitation energy used in our in situ investigation.

Figures 4 and 5 show the spectra recorded during in situ sample reduction, using 1 and 5% H_2, respectively, after redox treatments corresponding to various stages in the series of TPR profiles in Figure 2. Additional TPR experiments indicated that the difference in the final reduction temperature of Figure 5 with respect to Figure 2 does not affect the phenomena observed. All the initial spectra shown were recorded at 473 K, which are identical to those recorded at rt. These first spectra may therefore be considered as corresponding to Raman spectra *before* the TPR profiles 1−4 of Figure 2. During reduction with both 5 and 1% H_2, the first change observable in the Raman spectra with respect to the initial profiles is a decrease in the peak intensity, with no change in peak positions. The disappearance of the Raman bands occurs with the onset of sample reduction (compare Figure 2). However, it should be noted that the difference in experimental procedure (ramped vs stepped) should mean that, at a given temperature, the sample is more reduced in Figure 4 and 5 than in Figure 2. In parts A−D of Figure 4 and parts A−C of Figure 5, the intensities gradually disappear until featureless spectra are obtained. For the reduction process represented in Figure 5D, peak intensities at first decrease strongly between 573 and 623 K, after commencement of sample reduction, as in the other cases. However, at 773 K, a weak peak appears at 295 cm⁻¹, which becomes more intense and shifts to lower wavenumber as the temperature is increased, while others appear at 380 and 495 cm⁻¹. These peaks are consistent with formation of a
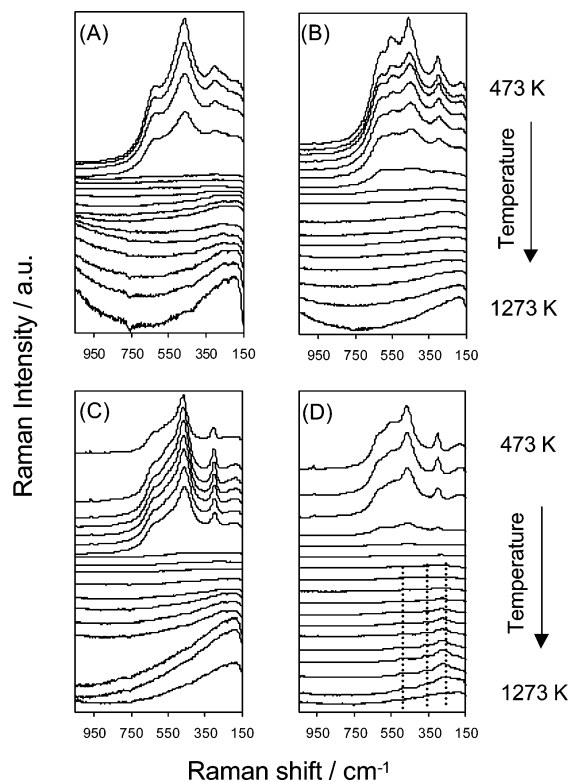
pyrochlore structure.[11] We have recently reported the same phenomenon for this sample using 10% H_2 as the reducing agent.[23] In the present case, the peaks attributable to the pyrochlore structure are somewhat less intense but nonetheless still very clear. As we pointed out previously, the most surprising aspect of this observation was the low temperature as pyrochlore formation is usually reported to form under much more severe reducing conditions.[7,10,11] In addition, the appearance of these peaks corresponds to the only reduction process of those shown in Figures 4 and 5, which occurs at low temperature (see Figure 2). Indeed, the lower temperature of reduction in Figure 5D with respect to parts of Figure 5A to C is also evident, as indicated by the temperature of onset of the decrease in intensity.

With regard to the structural information contained in the initial spectra, all exhibit multiple peaks between 150 and 750 cm⁻¹. Considering that a single Raman peak (F_{2g} at 465 cm⁻¹) is allowed for the fluorite structure, the splitting observed indicates a lowering of the symmetry in the coordination sphere of the oxygen atoms, i.e., a tetragonal transformation of the structure. On the basis of these data, it is impossible to determine whether the splitting corresponds to a lowering of the symmetry due to movement of the oxygen atoms from tetrahedral sites within a cubic cation lattice or to an actual tetragonal structure. Clearly, there are significant differences in the overall appearance of these spectra, thereby evidencing some structural differences. Previous reports of similar spectra, i.e., with variations in the relative intensities of the peaks, have been attributed to "some difference in the local displacement of oxygen atoms"
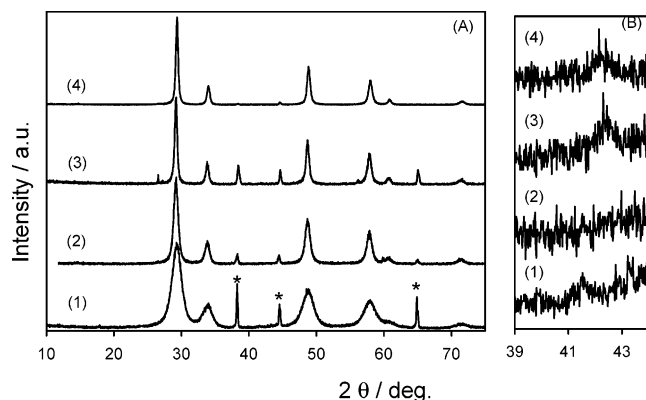
Figure 6. (A) XRD patterns of $Ce_2Zr_2O_8$ after: (1) CP; (2) SR−MO; (3) SR−MO−SR−SO; (4) SR−MO−SR−SO−SR−MO. CP, 773 K, 1 h; MO, 700 K, 1 h; SO, 2 h; SR, 5% H_2. The temperature of SO and SR is 1273 K in all cases. Sharp peaks at 2θ = 38.2, 44.4, and 64.8°, indicated by asterisks, are due to the sample holder. (B) The same as in A, over a restricted range with an increased acquisition time.

Table 1. Structural Data Obtained from XRD Patterns Shown in Figure 6 Using the Tetragonal ($P4_2/nmc$) Structural Model

sample[a]	a and b (Å)	c (Å)	V_{cell} (Å^3)
1	3.724(6)	5.32(1)	73.8(2)
2	3.729(3)	5.307(5)	73.8(1)
3	3.743(5)	5.324(9)	74.6(2)
4	3.726(1)	5.306(3)	73.69(6)

[a] Sample treatments are outlined in the caption of Figure 6.

or, in other words, to differences in degree of tetragonal distortion or displacement along the [001] direction.[10]

We find no clear correlation between the appearance of the initial spectra, or the trend in relative peak intensities, and the TPR profiles. As mentioned above, of the initial spectra shown, low-temperature reduction occurs only in the reduction following the first spectrum of 5D. This spectrum clearly shows a high degree of tetragonal distortion. However, this is also true of the first of 5B, which shows reduction at relatively high temperature. None of the spectra in which the F_{2g} mode of vibration predominates, which can be said to be closer to the cubic structure, show low-temperature reduction. This might indicate that tetragonal distortion favors reduction. On the other hand, on passing from A to B in both Figures 4 and 5, the sample clearly becomes more tetragonal, but the corresponding TPRs do not show an improvement in reduction performance (cf. profiles 1 and 2, Figure 2). Thus, the Raman spectra indicate very subtle structural differences, which can lead to strong differences in redox properties.

3.3. XRD. Further evidence of structural modification which may lead to a lowering in the temperature of reduction was sought by XRD. Figure 6A shows a series of XRD diffraction patterns obtained from $Ce_2Zr_2O_8$ after ex situ treatments corresponding to various stages of the TPR cycles indicated in Figure 2. The treatments employed correspond to the most severe conditions used in the TPR experiments and would be expected to result in more evident structural modification of the cation sublattice. Low-temperature reduction is observed only after the last of these treatments.

Estimation of the crystallite size from these XRD patterns show that high-temperature reduction results in an increase of the crystallite size from 5 nm (after CP, trace 1) to 11.3 (after the first SR−MO cycle, trace 2). Further crystallite size growth is induced by the SO procedure (21 nm, trace 3), with negligible change after the final treatment procedure (20 nm, trace 4). These results are in agreement with surface area measurements that indicate a decrease from 40 m^2 g^{-1} after CP to <10 m^2 g^{-1} after the other treatments.

The XRD patterns in Figure 6A exclude the occurrence of extensive phase separation in the sample. In view of the

fact that Raman spectra reveal some degree of tetragonalization for samples 1−4, which could indicate either the pseudocubic t″ or t′ structure, a more in-depth analysis of these profiles was conducted. Two characteristic features may in principle be used to distinguish between tetragonal and cubic structures. First, the 102 reflection at ca. $2\theta = 42°$ is allowed only for the tetragonal structure. Second, tetragonalization leads to splitting of reflections in the XRD patterns. As far as the 102 reflection is concerned, it should be noted that this peak has a low relatively intensity (1%) even in well-ordered structures. Thus, XRD data were carefully collected, by increasing the time of acquisition (12 s per step, in steps of 0.02°) and using a "zero background" holder made of a Si single crystal). Figure 6B shows the patterns thus obtained in the region around 42°. The presence of the 102 reflection is evident only after procedures 3 and 4.

Indications of peak splitting were also sought from an analysis of peak broadening of the peaks in Figure 6. The peak broadening observed was quite moderate, thereby ruling out strong tetragonalization. Thus, on the basis of all of the structural data, and in agreement with much of the available literature data, we attribute the structures after the last two treatments to t′ phases, with c/a values very close to 1. In the other two cases, the t″ structure cannot be ruled out.

Table 1 indicates structural parameters obtained by fitting the XRD patterns using the tetragonal ($P4_2/nmc$) model. These data indicate a slight increase in the cell volume after SO with respect to the reduced (and fresh) samples.

3.4. Formation of Pyrochlore. The characterization reported thus far indicates very similar structural features in all the samples, with no clear correlation between structure before reduction and temperature of reduction. The evidence of a pyrochlore-type structure by in situ Raman spectroscopy is the only factor that clearly distinguished the promoted material from the unpromoted material. Thus, pyrochlore formation was further investigated by analysis of aliquots of the sample after reduction at 1353 K−oxidation (aliquot 1), after SR−MO−SR−SO−SR−oxidation (aliquot 2), and after SR−MO−SR−SO−SR−MO−SR−oxidation (aliquot 3). In all cases, 5% H_2 was used as the reducing gas, SR and SO were conducted at 1273 K, and the last oxidation step was performed by exposure to air at rt. The aim of the high-temperature reduction treatment (1353 K) was to induce pyrochlore-type cation ordering,[11] to produce a reference for the other data. It should be remembered that the TPR of this sample shows a single, low-temperature reduction peak (Figure 2, profile 8). Aliquots 2 and 3 correspond to the material *before and after* promoted reduction.

The low temperature of oxidation was chosen in an attempt to preserve the effect of the reduction procedures. In a previous report, it was shown that reduction of a $Ce_2Zr_2O_8$

Pyrochlore Formation in Ce₂Zr₂O₈
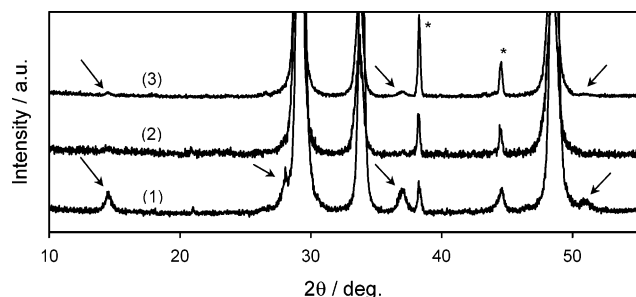
Chem. Mater., Vol. 17, No. 5, 2005 1163

Figure 7. XRD patterns of $Ce_2Zr_2O_8$ after the following treatments: (1) reduction at 1353 K (5 h)−oxidation (rt); (2) SR−MO−SR−SO−SR−oxidation (rt); (3) after SR−MO−SR−SO−SR−MO−SR−oxidation (rt). 5% H_2/Ar and 5% O_2/Ar were used. SR, 1273 K, 0.25 h; SO, 1273 K, 2 h; MO, 700 K, 1 h. Arrows indicate the peak positions characteristic of pyrochlore-type cation ordering.

Figure 8. Plot of fwhm vs 2θ for the diffraction peaks shown in Figure 7 for $Ce_2Zr_2O_8$ after reduction at 1353 K (5 h)−oxidation (rt). Peaks characteristic of pyrochlore type cation ordering are indicated by filled squares.

Figure 9. Raman spectra of samples of $Ce_2Zr_2O_8$ after the following treatments: (1) reduction at 1353 K (5 h)−rt oxidation; (2) SR−MO−SR−SO−SR−rt oxidation; (3) after SR−MO−SR−SO−SR−MO−SR−rt oxidation. 5% H_2/Ar and 5% O_2/Ar were used. SR, 1273 K, 0.25 h; SO, 1273 K, 2 h; MO, 700 K, 1 h; SO, 2 h.

sample at temperatures between 873 and 1573 K always results in a sample with a cubic structure.[11] However, subsequent oxidation at 873 K resulted in tetragonal systems for samples previously reduced between 873 and 1123 K. In cases where there was XRD evidence of pyrochlore formation under reducing conditions (between 1123 and 1573 K), oxidation at 873 K resulted in a general broadening and decrease in intensity of the peaks characteristic of cation ordering, unless this ordering was complete. Of particular relevance to the present work is the evidence that a sample which showed weak evidence of pyrochlore formation during reduction at 1123 K appeared to change to a tetragonal system on oxidation. Thus, oxidation at higher temperature may destroy evidence of pyrochlore-type cation ordering. However, a potential drawback of the low temperature of oxidation should be noted: it may not completely oxidize the sample, resulting in a significant Ce^{3+} content. This was in fact indicated by a green color of the three materials after rt oxidation.

The XRD patterns of these materials are shown in Figure 7. In the case of the sample reduced at 1353 K, weak peaks at 14 (111), 28 (311), 36 (331), and 52° (531) indicate the presence of κ- or pyrochlore-type cation ordering. The cation distribution is the same in the κ and pyrochlore phases,[26] so they give rise to similar main diffraction peaks. Notably, in the pyrochlore structure, the presence of Ce^{3+} ions leads to small shifts to lower diffraction angles. However, the presence of a pyrochlore phase after exposure to oxygen (even at rt) is unlikely. The reflections observed in Figure 7 are rather broad. This has been previously observed and attributed to incomplete cation ordering, giving rise to antiphase domain boundaries. Here, there is the added complication of the presence of both Ce^{3+} and Ce^{4+}. Interestingly, the peaks attributable only to the cation-ordered phase are systematically broader than those characteristic of the fluorite structure. Figure 8 shows a plot of the full width at half maximum (fwhm) vs 2θ for this sample. Clearly, the values for the cation-ordered peaks are systematically higher than those of the others. This observation suggests the presence of small pyrochlore domains nucleated within the fluorite matrix.

For aliquot 2, clear evidence for the characteristic peaks of a pyrochlore-type structure was not found (Figure 7, trace
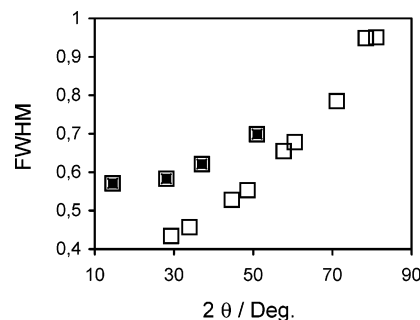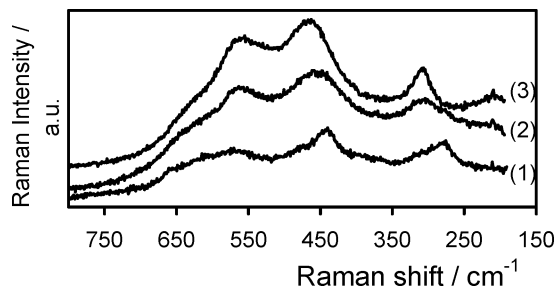
2). Close inspection suggests the possibility of the characteristic peaks, but they are very weak with respect to the noise and the assignment is somewhat inconclusive. In the case of aliquot 3, i.e., after promoted reduction, the characteristic peaks are evident, but they are very broad (Figure 7, trace 3). This indicates that the sample is not fully converted to a pyrochlore structure during promoted reduction. On one hand, this is perhaps unsurprising since higher temperature reduction did not completely convert the sample to pyrochlore (aliquot 1). On the other hand, the in situ Raman spectra indicate that perhaps more evidence could be expected. Thus, it appears that the oxidation step destroys the clear evidence of pyrochlore formation observed during the in situ Raman experiments.

The corresponding Raman spectra are shown in Figure 9. Raman spectroscopy provides information on the oxygen sublattice and therefore provides complimentary information on the structure to that revealed by XRD. The spectrum of aliquot 1 has similar features to the κ phase reported by Omata et al.,[10] which showed peaks at [172], 274, 437, and 570 cm⁻¹, with relatively intense shoulders at 306, 475, 602, [and 643] cm⁻¹. Here, the main peaks are at 275, 442, and 567 cm⁻¹, with high wavenumber shoulders on each. Other parallels exist with the structural data presented in that work. As in the present case, there was also evidence for antiphase boundaries. The authors indicated that κ is a cubic phase but with a lower symmetry than $Fd3m$ space group (that of pyrochlore).

More recently, the κ phase has been more thoroughly characterized. Kishimoto et al.[17] have suggested that the phase belonged to the $P2_13$ space group. Sasaki et al.,[21] however, in an electron diffraction study found a forbidden

(26) Hui, Z.; Nicolas, G.; Francoise, V.; Michele, P. *Solid State Ionics* **2003**, *160*, 317.

reflection, which casts some doubt on this assignment. The latter has found support from DFT calculations.[15] Sasaki et al. [21] also characterized a $Ce_2Zr_2O_{7.5}$ phase, obtained by rt oxidation of a pyrochlore structure. The authors concluded that this material was formed by ordered filling of half of the oxygen vacancies of the starting pyrochlore, resulting in a structure in the F43m space group (the minimal super-structure of the *Fd3m* space group). However, unlike the present data, in the above-mentioned reports, cation ordering was complete, or considered to be so, with little evidence of antiphase boundaries. The present data suggests the presence of small domains with cation ordering, which would almost certainly affect the reactivity with respect to a fully ordered matrix.

The other two spectra in Figure 9 are rather similar in appearance and may be assigned to a t′ phase, as for the spectra shown in Figures 4 and 5. Thus, although XRD revealed evidence for cation ordering in the case of aliquot 3, the Raman spectrum after rt oxidation does not correspond to the κ phase reported by Omata et al.[10]

3.5. Surface Characterization: Methanol Adsorption.
Methanol adsorption is a relatively sensitive technique which may be used to analyze the surface of CZMOs. After appropriate activation, methanol adsorbs dissociatively on the surface to complete the coordination sphere. Distinct peaks are observed for on-top methoxy species adsorbed on Ce^{4+} (1101 cm^{-1}) and Zr^{4+} (1156 cm^{-1}), which may be used to quantify the surface contribution of each cation.[27] This technique may be reliably used to obtain information on the overall surface composition and not on any surface arrangement, as the ν(OC)s of homocationic bridging species ($Ce^{4+}-Ce^{4+}$ and $Zr^{4+}-Zr^{4+}$) are difficult to distinguish from heterocationic bridging ($Ce^{4+}-Zr^{4+}$) species (all around 1058 cm^{-1}). The triply bridged species, which occurs at 1015 cm^{-1}, is of minor importance and appears as a very weak feature.[27]

Various samples, after different redox treatments, were analyzed by methanol adsorption. Analysis of a complete data set for comparison with the TPR profiles, in the same manner as the in situ Raman experiments, was somewhat hampered by the presence of bands due to residual bulk carbonate species after the first SR−MO treatment. These were superimposed on the methoxy species, which prevented clear observation of $Ce^{4+}-OCH_3$ and $Zr^{4+}-OCH_3$ signals. The SO treatment was necessary for their complete elimination. The negligible presence of these features in the spectrum of the fresh sample is most probably due to the high surface-to-bulk ratio. Thus, analysis is reported only for the sample subjected to the following treatment: CP, SR−MO−SR−SO, and SR−MO−SR−SO−SR−MO, using both 1 and 5% H$_2$. The results are shown in Figure 10 and Table 2. Previous reports, using a series of high surface area samples, have indicated that the intensity of methoxy species adsorbed on Zr^{4+} shows a linear dependence on the mole fraction of zirconium in the mixed oxide.[28] The intensity of the $Zr^{4+}-OCH_3$ feature (1155 cm^{-1}) on the sample may thus
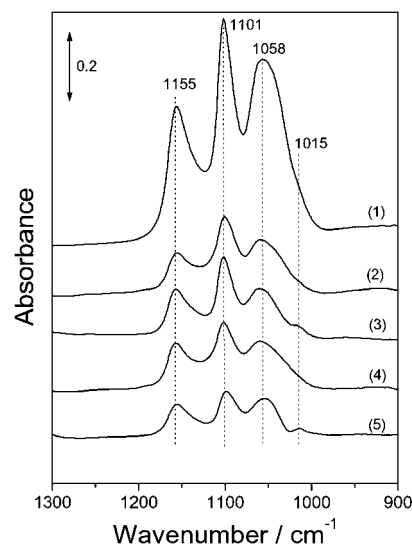

Figure 10. FTIR spectra of methanol adsorption after: (1) after CP; (2) after SR−MO−SR−SO (1% H$_2$); (3) after SR−MO−SR−SO−SR−MO (1% H$_2$); (4) after SR−MO−SR−SO (5% H$_2$); (5) SR−MO−SR−SO−SR−MO (5% H$_2$). CP, 773 K, 1 h; MO, 700 K, 1 h; final temperature of SR and of SO = 1173 (1% H$_2$) or 1273 (5% H$_2$).

Table 2. Relative Intensities of the $Ce^{4+}-OCH_3$ and $Zr^{4+}-OCH_3$ Signals for the Spectra Shown in Figure 10

sample pretreatment	I_{Ce}/I_{Zr} (1% H$_2$)	I_{Ce}/I_{Zr} (5% H$_2$)
CP		1.48
SR−MO−SR−SO	1.80	1.33
SR−MO−SR−SO−SR−MO	1.62	1.29

be used to calculate the surface concentration of Zr^{4+} and therefore also of Ce^{4+} ($Ce^{4+}-OCH_3$ at 1101 cm^{-1}). However, in view of the low surface areas of samples treated at high temperature, the error in this variable would be significant, thereby leading to a relatively large error in surface concentration. Thus, in Table 2, the relative intensities of the $Ce^{4+}-OCH_3$ and $Zr^{4+}-OCH_3$ species are used to estimate changes in surface concentration induced by the various procedures.

With respect to the initial surface, significant changes in the surface composition are evident. Thus, in the case of the sample treated with 1% H$_2$, there is considerable enrichment in cerium, while in the case of the sample treated with 5% H$_2$ the sample surface becomes enriched in zirconium. This might suggest that surface zirconium enrichment favors promotion of reduction. However, a straightforward correlation between surface composition and the further promotion of reduction which is the subject of the present study (e.g., more zirconium = promoted reduction) is not evidenced by the present data. In brief, this may be concluded from the observation that the two samples treated with 5% H$_2$ show almost identical surface composition (C and D), yet one is promoted and the other is not. Furthermore, such a conclusion would be difficult to rationalize in comparison with the open literature as both zirconium-[29] and cerium-rich compositions[13] show the ability to undergo promoted reduction.

The main conclusion of this methanol adsorption study is that surface cation rearrangement can occur under the conditions employed here.

(27) Daturi, M.; Binet, C.; Lavalley, J. C.; Galtayries, A.; Sporken, R. *PCCP* **1999**, *1*, 5717.
(28) Daturi, M.; Finocchio, E.; Binet, C.; Lavalley, J. C.; Fally, F.; Perrichon, V. *J. Phys. Chem. B* **1999**, *103*, 4884.

(29) Kaspar, J.; Di Monte, R.; Fornasiero, P.; Graziani, M.; Bradshaw, H.; Norman, C. *Top. Catal.* **2001**, *16*, 83.

Pyrochlore Formation in Ce₂Zr₂O₈

Chem. Mater., Vol. 17, No. 5, 2005 1165

3.6. Origin of Low-Temperature Reduction. The TPR investigation in the present study indicates how the reduction profile is influenced by redox treatments. The $Ce_2Zr_2O_8$ material studied shows a single high-temperature reduction peak when the prior redox treatments are not very severe. When more severe redox treatments are applied, TPRs show two-peak profiles (although within these two peaks shoulders are evident). Reduction at 1353 K induces a single low-temperature TPR peak.

The main conclusions of the structural investigation into the origin of this TPR behavior may be summarized as follows:

(1) Before all of the TPR profiles, the structural data are consistent with the presence of t″ phases or t′ phases with c/a close to 1. Variations in the degrees of local displacement in the anion sublattice are also evident (Figures 4−6).

(2) Evidence of pyrochlore-type cation ordering was not found before the promoted TPR (Figures 7 and 9).

(3) Evidence for pyrochlore-type cation ordering in the sample after the promoted TPR is clearly suggested by XRD. However antiphase boundaries are also present (Figure 7). Oxidation at 700 K instead of rt destroys this evidence for cation ordering.

(4) Increasing the temperature of reduction to 1353 K evidenced significant cation ordering (Figure 7). However antiphase boundaries are also present (Figures 7 and 8).

(5) Methanol adsorption studies indicate that surface cation reordering is observed under the treatment conditions employed (Figure 10).

None of these materials show complete cation ordering, yet promotion of reduction is apparent. Thus, the data unequivocally show that bulk pyrochlore formation is not a necessary precondition to observe low-temperature reduction. Even partial ordering results in promotion of reduction. In our previous report,[23] we proposed that pyrochlore-type cation ordering was initiated before the promoted TPR and continued at lower temperature during the TPR, given that the kinetics of the transformation have not been reported. Although we have no direct evidence of the presence of ordering before the promoted TPR, we believe that this offers the most reasonable explanation of the effects reported here. The extent of such ordering for our sample before promotion must be below the detection limit of the XRD technique. For this reason we turned our attention to the surface. The results of methanol adsorption indicate that surface reordering occurs. On the basis of the present results, it is not possible to determine the extent of surface ordering. However, on the basis of the observation that the promoted sample has a similar composition to an unpromoted sample, we believe that the phenomenon does not concern the whole surface. A further consideration is that promotion of reduction has been observed for other compositions.[13,29] In such cases, complete cation ordering is not possible, being limited by one or another of the cations in the mixed oxide.

An outstanding question is the extent of the ordering which takes place during promoted reduction. In situ Raman show only pyrochlore during the reduction, which suggests that the transformation may be quite significant. However, after oxidation at rt, XRD shows only weak evidence of pyrochlore

peaks, while the Raman spectrum indicates a t′ and not a κ phase. The evidence for the sample reduced at 1353 K shows that, when the ordering is more extensive but incomplete, it is visible by both techniques after rt oxidation. Thus, in agreement with data reported elsewhere, it is more difficult to detect evidence for cation ordering when antiphase boundaries are present. As indicated above, average or predominant structures are detected in such cases. However, it may be concluded that the extent of transformation during TPR does not arrive to the extent of ordering induced by reduction at 1353 K.

Given that even partial ordering leads to promotion of reduction, it is of potential importance to note that, at least on the basis of Raman evidence, low-temperature pyrochlore formation during reduction does not occur for 1% H_2, it does for 5% H_2 and is more evident for 10% H_2.[23] The extent of promotion observed in the TPR profiles depends on the concentration of H_2 in the same way as this evidence for pyrochlore-type ordering during reduction. In addition, the sample with the most extensive cation ordering exhibits a single low-temperature peak in the TPR profile. Thus, the TPR promotion may be linked to the extent of pyrochlore-type ordering before the TPR. As the extent increases, the TPR moves from a single high-temperature peak to a single low-temperature peak, through various intermediate stages. The transformation may be seen as a pathway between two structures (t′ and κ), the initial steps of which are illustrated by the initial changes in the TPR profile. The data also suggests that the extent of cation ordering achieved depends on the severity of the conditions, which in turn suggests that kinetic factors do in fact play an important role in these transformations.

The importance of cation ordering is an issue which is beginning to receive some attention for CZMOs.[15,18] Conesa[15] has recently underlined that, while often ignored in analysis of these materials, such effects are potentially of considerable importance. That work points out that many different arrangements are possible, which have different energies and which are strongly influenced by the initial preparation procedures and subsequent treatments. The κ phase is cited as the least stable of the wide range of structures investigated. On the basis of literature evidence, the κ phase unquestionably leads to reduction at low temperature. In situations where ordering is incomplete, such as after the promoted TPR in the present work, extended ordered and disordered regions must exist if they can be detected by XRD. The ability of even limited cation ordering (and not bulk formation) to promote reduction is a point of enormous potential interest. The work of Conesa provides an interesting insight in this regard. Although concerned with bulk structure, the DFT calculations performed indicate that, if the characteristics possessed by the atoms in this arrangement are maintained at the surface, the simultaneous presence of stronger Lewis acid and basic sites might expected. Our belief is that pyrochlore-type cation ordering at the surface results in sites which promote reduction, perhaps through hydrogen activation. Interestingly, we have previously reported that the lowest H−D scrambling temperature of the four samples in Figure 6 is shown by this sample after SO−

SR(5% H_2)−MO, that is, after the sample treatment which results in low-temperature reduction.[12]

4. Conclusions

The main conclusions of the present investigation may be summarized as follows:

(1) The temperature of reduction of $Ce_2Zr_2O_8$ is strongly affected by application of severe oxidizing and reducing cycles. The redox treatments are mutually interdependent: to produce an effect, the severity necessary for the reducing treatment shows a dependence on the severity of oxidizing part of the cycle. The TPR profile may be varied from a single high-temperature peak (after SO), through a high and low-temperature two-peak profiles, to a single-peak low-temperature profile (after subsequent SR−MO);

(2) Structural analysis suggests that the behavior depends on pyrochlore-type ordering in the cation lattice. The relative ease of reduction of the κ-phase (produced by low-temperature oxidation of the pyrochlore phase) is confirmed. However the data also indicates that bulk pyrochlore formation is not a necessary condition to observe its effect. Two-peak TPR profiles are observed when cation ordering is incomplete.

CM0481574